Journal of Materials Chemistry A

RSC Publishing

COMMUNICATION

View Article Online
View Journal | View Issue

Cite this: J. Mater. Chem. A, 2013, 1, 9414

Received 16th February 2013
Accepted 15th March 2013

DOI: 10.1039/c3ta10710h

www.rsc.org/MaterialsA

Fluorination of "brick and mortar" soft-templated graphitic ordered mesoporous carbons for high power lithium-ion battery†

Pasquale F. Fulvio,[a] Gabriel M. Veith,[b] Jamie L. Adcock,[c] Suree S. Brown,[c] Richard T. Mayes,[a] Xiqing Wang,‡[a] Shannon M. Mahurin,[a] Bingkun Guo,[a] Xiao-Guang Sun,[a] Alex A. Puretzky,[d] Christopher M. Rouleau,[d] David B. Geohegan[d] and Sheng Dai*[ac]

Ordered mesoporous carbon–graphitic carbon composites prepared by the "brick and mortar" method were fluorinated using F_2 and investigated as cathodes for primary lithium batteries. The resulting materials have a rich array of C–F species, as measured by XPS, which influence conduction and voltage profiles.

CF_x batteries have the highest energy density among all primary lithium batteries (250 W h kg^{-1}).[1,2] The fluorination of the carbon materials generates surface species, such as $-CF_2$/$-CF_3$ groups which react with the Li-ions. Consequently, the specific capacity of the cells increases with fluorine contents.[2–4] Currently available Li/CF_x batteries are limited to low rate applications due to their poor electronic conductivity and the layered nonporous structure of the graphite cathode precursor.[5]

For materials having graphitic structures, extreme temperatures and catalysts are required to obtain high F/C ratios due to their low initial surface areas. For instance, partially exfoliated graphitic carbon fibers with F/C ratios of 0.86 were obtained only after treatment at 480 °C.[4,6] Migrating from traditionally used graphitic materials towards porous carbons substrates is an attractive alternative in order to obtain highly fluorinated carbon materials using milder conditions. A recent example was demonstrated for CMK-1 ordered mesoporous carbon (OMC) prepared as inverse replicas of ordered mesoporous silica (OMS) MCM-48.[7] Fluorinated OMCs with F/C ratios between 0.1 and 0.5 were obtained using elemental fluorine at temperatures ranging from room temperature to 150 °C, much lower than those for graphite (>400 °C).[8] For higher F/C ratios of 0.8 prepared at 250 °C, however, the mesopore structure was lost during fluorination.[8] In order to overcome stability issues, phenolic or novolak based soft-templated carbons using triblock copolymers of general formula poly(ethylene oxide)-poly(propylene oxide)-poly(ethylene oxide), PEO-PPO-PEO,[9] have been recently fluorinated before and after chemical activation. Mesopores of the latter carbons were largely retained even at F/C ratios of 0.8 and higher, whereas fluorination temperatures were kept below 250 °C.[10]

In general, these soft-templated carbons display poor electronic conductivities.[11] After extensive fluorination, only a small fraction of the conductive carbon backbone is preserved, which further lessens the conductivity and voltages of these materials. Consequently, lower discharge potentials and Li-capacities of fluorinated carbons at high discharge rates are obtained when tested as primary Li-ion battery cathodes.[10] In order to improve the electronic conductivity of soft-templated carbons without using high temperature graphitization, a "brick and mortar" method was developed.[11]

This method was originally developed for metal oxides,[12] in which a metal alkoxide "mortar" was self-assembled with crystalline oxide nanoparticles and triblock copolymers, being then extended to porous carbon–graphitic carbon systems. In the latter case, the "mortar" was a soft-templated OMC and the graphitic "bricks" were carbon black (CB), onion-like carbons (OLCs) and multi-walled carbon nanotubes (MWNT).[11] Nanocomposites exhibited well-developed mesopores, high surface areas, graphitic domains and higher electronic conductivity compared to standard OMCs, making these ideal candidates for supercapacitor and rechargeable Li-ion battery electrodes.[11] Despite the many advantages offered by this type of nanocomposites, the ability to fluorinate the OMC "bricks" while preserving large fractions of the graphitic "bricks" to ensure higher electronic conductivity have not been demonstrated yet.

[a]Chemical Sciences Division, Oak Ridge National Laboratory, Oak Ridge, Tennessee 37831, USA. E-mail: dais@ornl.gov; Fax: +1-865-576-5235; Tel: +1-865-576-7307
[b]Materials Science and Technology Division, Oak Ridge National Laboratory, Oak Ridge, Tennessee 37831, USA
[c]Department of Chemistry, University of Tennessee, Knoxville, Tennessee 37996, USA
[d]Center for Nanophase Materials Sciences, Oak Ridge National Laboratory, Oak Ridge, Tennessee 37831, USA

† Electronic supplementary information (ESI) available: Detailed experimental and relevant references, Table S1 with summary of calculated N_2 adsorption parameters and Table S2 XPS results, Fig. S1 with N_2 isotherms for fluorinated graphitic nanoparticles, Fig. S2 with additional C1s and F1s XPS spectra, Fig. S3. See DOI: 10.1039/c3ta10710h

‡ Present address: Nanotek Instruments, Inc., Dayton, Ohio 45404, USA.

Herein, various OMC–graphitic carbon nanocomposites with CB, MWNT, single walled carbon nanohorns (SWNHs) and graphene nanoplatelets (GnPs) were prepared similar to previous reports[11] and then fluorinated after carbonization, see ESI† for detailed experimental. Materials were labeled according to graphitic nanostructure added to the OMC precursor and their percentage in the synthesis gel of 10 or 25 wt%, *i.e.* GnP-25/F meaning fluorinated OMC–graphene nanocomposite having 25 wt% GnP prior to carbonization.

Representative SEM images of CB-25 and GnP-25 prior to fluorination are shown in Fig. 1A and B, respectively. These show an OMC film coating GnP platelets with horizontally aligned cylindrical mesopores, in contrast to the former composite in which CB particles are dispersed throughout a bulk OMC framework. Similarly to GnP-*x* samples, thinner OMC "mortar" is seen SWNH-*x* materials, whereas bundles of MWNTs are distributed within the OMC framework (not shown). N_2 −196 °C isotherms, Fig. 1C, are type IV[13] with capillary condensation steps at high relative pressures. These are typical of materials with large mesopores,[13] as confirmed by the corresponding pore size distributions (PSDs),[14] Fig. 1D. These isotherms and PSDs of the fluorinated materials largely resemble those of the starting carbons. Summarized data for materials before and after fluorination is provided in Table S1 in ESI.† The total pore volume and specific surface areas for fluorinated samples were 40 to 50% lower than their starting materials. Whereas the mesopore widths were essentially unchanged by the fluorination process thus, showing the high chemical stability of these nanocomposites. Finally, the SWNH brick exhibited small amounts of micropores after fluorination, see Table S1 and Fig. S1 in ESI.† Similarly, previous studies on the fluorination of SWNHs at 200 °C demonstrated that some of the SWNHs were opened during reaction with F_2.[15] Hence, the interior of the fluorinated SWNHs became accessible, consequently increasing the pore volumes and specific surface areas.

Analysis of the X-ray photoelectron spectroscopy (XPS) measurements revealed that the composites surface chemistry was dominated solely by C and F species, without evidence of surface oxygen. Elemental analysis data shows that all the samples have roughly the same C–F ratio (~44 : 56 at.% C : F), with the exception of the GnP-25 which only has ~32 at.% F, thus, confirming the chemical robustness of graphene.

Investigating the C1s spectra collected for the 4 samples reported in this work reveals a rich surface chemistry, see Fig. 2A and S2 in ESI.† These materials display a combination of nine different C–F species observed between the samples. Also interesting, the fraction and type of surface moieties varied significantly from sample to sample despite the large fraction of OMC "mortar" within these materials. For example, three of the fluorinated graphitic "bricks", namely CB/F, SWNH/F and MWNT/F had evidence for $FC(C)_3$ species (288.8 eV). However the concentration varied from 6 to 53% of the total C species on the composites surface. This wide variation in chemistry indicates that the surface curvature, presence and types of defects in the starting "bricks" play a significant role in the reactivity with the F_2 gas,[16] and that the OMC "mortar" does not lead to the same surface functionality.

Analysis of the F1s data, see representative spectra in Fig. 2B and S2,† again revealed a wide variation in surface F species. All of the samples contained semi-ionic type F (688 eV). However, the SWNH-25/F sample also contained high levels (8 at.%) of ionic C–F bonds. These ionic bonds, as discussed below, result in higher cell potentials compared to the other materials.[10] In addition to the ionic and semi-ionic chemistry there is evidence in the SWNH and GnP based materials of the presence of strongly covalent C–F chemistry (691 eV). Furthermore, as a consequence of the strong covalent character of the C–F bonds in SWNH, CF_4 species may have formed upon fluorination of SWNH. The CF_4 may have remained trapped in the nanocomposite material with highest percentage of graphitic brick, namely SWNH-25/F. This species was not present in SWNH-10/F material, possibly because of the restricted access of F_2 to the graphitic "brick" by F_2, which is more hindered by the OMC "mortar".

The carbon–fluorine composites were electrochemically reacted with Li, Fig. 3. All of the samples, with the exception of SWNH-25/F, have initial discharge potentials around 2.75 V.

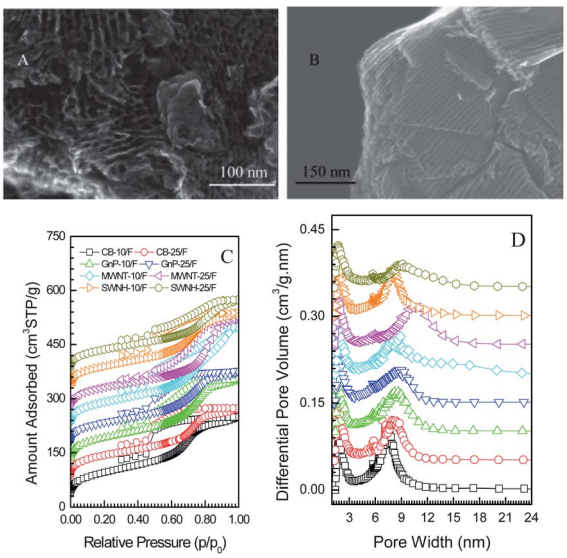

Fig. 1 SEM images of CB-25 (A) and of GnP-25 (B) nanocomposites, respectively, before fluorination; N_2 −196 °C isotherms (C) and corresponding pore size distributions (D) for fluorinated nanocomposites.

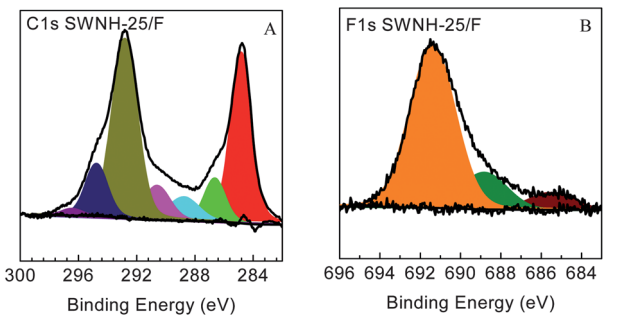

Fig. 2 Representative C1s (A) and F1s (B) spectra of SWNH-25/F material.

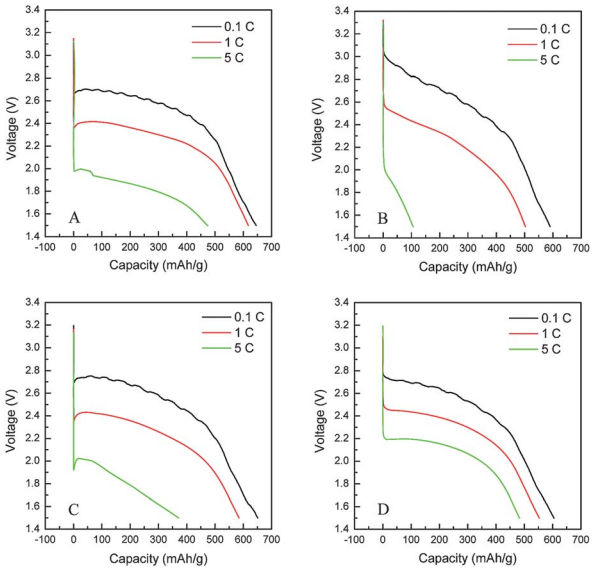

Fig. 3 Discharge profiles of CB-25/F (A), SWNH-25/F (B), MWNT-25/F (C) and GnP-25/F (D) at different discharge rates.

The SWNH-25/F material has a higher initial potential (3.0 V) due to the presence of ionic C–F bonds evidenced in the XPS data.[10] The materials all exhibit sloping discharge profiles with capacities around 600–650 mA h g^{-1} at a discharge rate of 0.1 C (10 hour discharge rate). The sloping profile likely originates from the wide variation in C–F functionality in these materials and rates of diffusion to these different reaction sites.

Surprisingly there are significant variations in discharge capacity and voltage when the materials are lithiated at a higher rate (5 C). Indeed, at this higher rate the voltage of all the cells decreases to 2.0 V with the exception of the GnP material which is significantly higher (2.2 V). This increase in cell voltage is likely attributed to higher electron conductivity. This hypothesis can be confirmed from the analysis of sp^2 type C–C bonds evident in the C1s data (C–C – 284.8 eV; $C(C)_2(CF)$ – 286.0 eV). The GnP sample has approximately 26% of the C species in the more conductive sp^2 state while the MWNT and CB samples contain only about 18% of the sp^2 carbon. The SWNH sample is likely more resistive due to the ionic C–F bonds. The relatively constant Li capacity between these four materials is curious considering the wide variation in C–F stoichiometry, Table S2.† It is likely that the MWNT, SWNH, and CB samples have more electrically isolated C–F species lowering the probability of reacting with a Li-ion while the more conductive GnP access more of the available reactive sites. Supporting that are the initial potential dips related to overvoltage for fluorinated carbons due to their insulating behavior.[17] Such dips in the potential are absent in case of GnP-25/F electrode material, which instead, displays a flat plateau, due to its higher electron conductivity. Finally, the electrical impedance spectroscopy (EIS) for these materials was measured before discharge (Fig. S3†). These curves show that the cell with GnP-25/F as the active cathode material has a series resistivity of ~3.5 ohms, lower than all others samples, approximately 5.0 ohms. Clearly, C and F chemistry will play a major role in the total capacity of the electrochemical cell and optimizing these species will lead to higher capacity and energy density materials.

In summary, OMC–graphitic carbon nanocomposites with various graphitic nanostructures were fluorinated. Various types of C–F bonds were identified for all samples. For SWNH composites, ionic C–F bonds were identified, thus accounting for their higher Li-discharge potentials but lower capacities at higher rates when tested as Li/CF_x electrodes. On the contrary, the backbone of GnP materials have higher concentrations of sp^2 carbon resulting in more stable discharge profiles at high Li-discharge rates. These results are promising for the development of energy storage and conversion devices requiring high power and energy densities.

This work was supported by the U.S. Department of Energy's Office of Basic Energy Science, Division of Materials Sciences and Engineering. PF and SM in synthesis of mesoporous carbons were supported by the Fluid Interface Reactions, Structures, and Transport (FIRST) Center, an Energy Frontier Research Center funded by the U.S. Department of Energy, Office of Science, Office of Basic Energy Sciences. A portion of this research was performed at the Center for Nanophase Materials Sciences which is sponsored at Oak Ridge National Laboratory by the Scientific User Facilities Division, Office of Basic Energy Sciences, U.S. Department of Energy.

Notes and references

1 T. Nakajima, *J. Fluorine Chem.*, 1999, **100**, 57; D. Linden, *Handbook of Batteries*, McGraw-Hill, 1994, vol. 2.
2 T. Nakajima, H. Touhara and F. Okino, *Actual. Chim.*, 2006, 119.
3 K. Naga, T. Nakajima, S. Aimura, Y. Ohzawa, B. Zemva, Z. Mazej, H. Groult and A. Yoshida, *J. Power Sources*, 2007, **167**, 192; T. Nakajima, S. Shibata, K. Naga, Y. Ohzawa, A. Tressaud, E. Durand, H. Groult and F. Warmont, *J. Power Sources*, 2007, **168**, 265.
4 R. Yazami, A. hamwi, K. Guerin, Y. Ozawa, M. Dubois, J. Giraudet and F. Masin, *Electrochem. Commun.*, 2007, **9**, 1850.
5 P. Lam and R. Yazami, *J. Power Sources*, 2006, **153**, 354.
6 F. Chamssedine, M. Dubois, K. Guerin, J. Giraudet, F. Masin, D. A. Ivanov, L. Vidal, R. Yazami and A. Hamwi, *Chem. Mater.*, 2007, **19**, 161.
7 R. Ryoo, S. H. Joo and S. Jun, *J. Phys. Chem. B*, 1999, **103**, 7743; R. Ryoo, S. H. Joo, M. Kruk and M. Jaroniec, *Adv. Mater.*, 2001, **13**, 677.
8 Z. J. Li, G. D. Del Cul, W. F. Yan, C. D. Liang and S. Dai, *J. Am. Chem. Soc.*, 2004, **126**, 12782.
9 Y. Meng, D. Gu, F. Q. Zhang, Y. F. Shi, L. Cheng, D. Feng, Z. X. Wu, Z. X. Chen, Y. Wan, A. Stein and D. Y. Zhao, *Chem. Mater.*, 2006, **18**, 4447; Y. Meng, D. Gu, F. Q. Zhang, Y. F. Shi, H. F. Yang, Z. Li, C. Z. Yu, B. Tu and D. Y. Zhao, *Angew. Chem., Int. Ed.*, 2005, **44**, 7053; F. Q. Zhang, Y. Meng, D. Gu, Y. Yan, C. Z. Yu, B. Tu and D. Y. Zhao, *J. Am. Chem. Soc.*, 2005, **127**, 13508; X. Q. Wang, C. D. Liang and S. Dai, *Langmuir*, 2008, **24**, 7500; C. D. Liang and S. Dai, *J. Am. Chem. Soc.*, 2006, **128**, 5316.

10 P. F. Fulvio, S. S. Brown, J. Adcock, R. T. Mayes, B. Guo, X.-G. Sun, S. M. Mahurin, G. M. Veith and S. Dai, *Chem. Mater.*, 2011, **23**, 4420.

11 P. F. Fulvio, R. T. Mayes, X. Wang, S. M. Mahurin, J. C. Bauer, V. Presser, J. McDonough, Y. Gogotsi and S. Dai, *Adv. Funct. Mater.*, 2011, **21**, 2208; B. Guo, X. Wang, P. F. Fulvio, M. Chi, S. M. Mahurin, X.-G. Sun and S. Dai, *Adv. Mater.*, 2011, **23**, 4661.

12 J. M. Szeifert, D. Fattakhova-Rohlfing, D. Georgiadou, V. Kalousek, J. Rathousky, D. Kuang, S. Wenger, S. M. Zakeeruddin, M. Gratzel and T. Bein, *Chem. Mater.*, 2009, **21**, 1260.

13 M. Kruk and M. Jaroniec, *Chem. Mater.*, 2001, **13**, 3169.

14 M. Jaroniec and L. A. Solovyov, *Langmuir*, 2006, **22**, 6757; J. Choma, J. Gorka and M. Jaroniec, *Microporous Mesoporous Mater.*, 2008, **112**, 573.

15 Y. Hattori, H. Kanoh, F. Okino, H. Touhara, D. Kasuya, M. Yudasaka, S. Iijima and K. Kaneko, *J. Phys. Chem. B*, 2004, **108**, 9614.

16 W. Zhang, M. Dubois, K. Guerin, P. Bonnet, H. Kharbache, F. Masin, A. P. Kharitonov and A. Hamwi, *Phys. Chem. Chem. Phys.*, 2010, **12**, 1388.

17 Y. Li, Y. Chen, W. Feng, F. Ding and X. Liu, *J. Power Sources*, 2011, **196**, 2246; M. Dubois, K. Guérin, W. Zhang, Y. Ahmad, A. Hamwi, Z. Fawal, H. Kharbache and F. Masin, *Electrochim. Acta*, 2012, **59**, 485.